

Short Communication

Template Synthesis of Hollow MoS₂ Microspheres with Enhanced Electrocatalytic Activity for Hydrogen Evolution

Bin Dong^{1,2,*}, Guan-Qun Han^{1,2}, Wen-Hui Hu¹, Yan-Ru Liu¹, Xiao Li¹, Xiao Shang¹, Yong-Ming Chai^{1,*}, Yun-Qi Liu¹, Chen-Guang Liu^{1,*}

¹ State Key Laboratory of Heavy Oil Processing, China University of Petroleum (East China), Qingdao 266580, PR China

² College of Science, China University of Petroleum (East China), Qingdao 266580, PR China

*E-mail: dongbin@upc.edu.cn (B. Dong), ymchai@upc.edu.cn, cgliu@upc.edu.cn (C.-G. Liu)

Received: 6 November 2015 / Accepted: 5 January 2016 / Published: 1 March 2016

Novel hollow MoS₂ microspheres with enhanced electrocatalytic activity for hydrogen evolution reaction (HER) have been synthesized by a facile self-sacrificial template method using MnCO₃ spheres as precursor. During a hydrothermal sulfuration process, uniform MnCO₃ spheres transformed to MoS₂/MnS core-shell structures. After removal of MnS with acid treatment of MoS₂/MnS, hollow MoS₂ microspheres have been obtained. XRD show that pure MoS₂ has been synthesized without any impurity. SEM images show that hollow MoS₂ structure is spherical morphology and consisted of many MoS₂ nanosheets, which imply more exposed edges and rims of MoS₂ nanosheets. The electrocatalytic activity of hollow MoS₂ microspheres for HER has been investigated. The results show that hollow MoS₂ microspheres have better activity for HER than conventional MoS₂ nanoparticles, which imply that hollow MoS₂ structures have more active sites for HER. Template synthesis of hollow MoS₂ microspheres is a suitable choice for high active electrocatalysts.

Keywords: template synthesis; hollow MoS₂ microspheres; hydrogen evolution; electrocatalytic activity

1. INTRODUCTION

Owing to the increasing energy needs, it is a great challenge to develop the renewable energy sources [1]. Hydrogen energy has been widely investigated as one of the most promising energy carriers for effectively utilizing the intermittent sustainable resources such as solar energy, tide energy, waterpower, wind energy and so on [2-4]. Hydrogen evolution reaction (HER) has recently attracted considerable attention as an effective way for water splitting by electrocatalysis [5-6] or

photoelectrocatalysis [7]. The electrocatalytic HER needs electrocatalysts with highly catalytic activity to lower its overpotential and accelerated the rate of water splitting [8]. Pt-based catalysts have been proved to be the most remarkable electrocatalysts for HER. However, the expensive cost and limited reserves of Pt-based catalysts have limited the industrial utilization on hydrogen evolution [9]. Therefore, the substitute materials with low price and earth-abundant reserves have become a hot research.

Among many substitute materials, the computational computation and experimental research have proved that molybdenum disulfides (MoS_2) demonstrated the promising electrocatalytic properties for HER [10-11]. Due to analogous layered structure of graphene, 2-D MoS_2 nanosheets are facile to restack and decrease the effective surface area. On the other hand, the electrocatalytic activity of MoS_2 largely depends on the number of the active sites, which are mainly on the rims and edges of MoS_2 nanosheets [12]. Therefore, designing novel MoS_2 three-dimensional (3D) nanostructures with more catalytic active sites may be a suitable choice to reduce the harmful impact of aggregation derived from 2D nanosheets. In fact, all kinds of MoS_2 -based hybrid nanostructures have been prepared using different substrates, such as carbon nanotubes [13], carbon spheres [14], TiO_2 nanosheets [15], graphene [16-17]. These hierarchical structures have provided more active sites and avoided severe aggregation of nanosheets. Recently, MoS_2 -based hierarchical hollow nanostructures with low density and high area surface have attracted great interest on the fields such as catalysis [18] or lithium-ion batteries [19]. Notwithstanding these researches, the synthesis of hollow structures of MoS_2 has still been a challenge owing to the high surface energy and aggregation of 2D nanosheets [20-21].

In this work, we have adopted facile self-sacrificial template synthesis using MnCO_3 spheres as template to prepare hollow MoS_2 microspheres. Firstly, uniform MnCO_3 spheres have been synthesized as template. Secondly, a facile sulfuration process has been used to prepare MoS_2/MnS shell/core hybrid structures. Finally, with the removal of MnS spheres template by acid treatment, hollow MoS_2 microspheres have been obtained, which have demonstrated enhanced electrocatalytic activity for HER.

2. EXPERIMENT SECTION

2.1 Preparation of MnCO_3 microspheres

Based on the previous literature [22], MnCO_3 microspheres were synthesized. Typically, solution A was obtained by dissolving the manganese sulphate (3 mmol) into the mixed solvent (21 mL ethanol and 210 mL de-ionized water). Solution B was formed by dissolving sodium hydrogen carbonate (30 mmol) in the de-ionized water (210 mL). Solution B was added into solution A. Then, the mixed solution was stirred vigorously at room temperature for 3 h. Then, the obtained MnCO_3 microspheres were collected by filtration, washed with de-ionized water and ethanol for several times, and dried at room temperature.

2.2 Preparation of MoS₂/MnS core-shell microspheres

0.40 g of as-prepared MnCO₃ microspheres was added into 80 mL de-ionized water and stirred for 30 min. Then, 0.6 g sodium molybdate (Na₂MoO₄ · 2H₂O) and 2.5 g L-cysteine were dissolved into the above solution. After stirring for 30 min, the solution was transferred to a 100 mL Teflon-lined autoclave, sealed and maintained at 220 °C for 24 h. The autoclave was cooling to room temperature naturally. Then the obtained samples were filtered, washed with deionized water and absolute alcohol several times, and then dried at 80 °C for 12 h in a vacuum oven.

2.3 Preparation of hollow MoS₂ microspheres

40 mg of the above MnS₂/MnS microspheres were added in 80 mL of 0.2 M HCl and stirred at room temperature for 24 h. Then the MnS cores were removed. The obtained black precipitates were rinsed with deionized water for several times until the solution becomes neutral, and dried at 60 °C for 12 h in a vacuum oven.

2.4 Physical characterization

XRD was performed on a panalytical X'pert PROX-ray diffractometer with Cu K α monochromatized radiation ($\lambda=1.54$ Å) and operated at 45 kV and 40 mA. The scan rate was 8 min⁻¹ and the 2 θ scan range was from 5° to 76°. TEM was performed on a JEM-2100 UHR microscope (JEOL, Japan) at an accelerating voltage of 200 kV. The morphology of the samples was examined with field-emission scanning electron microscopy (SEM, Hitachi, S-4800). XPS was performed on a VG ESCALABMK II spectrometer using an Al K α (1486.6 eV) photon source. The Brunauer-Emmett-Teller (BET) specific surface areas were determined by nitrogen sorption isotherms that were measured on a ChemBET 3000 (Quantachrome, USA) instrument to obtain the surface areas.

2.5 Evaluation of Electrocatalytic Activity toward HER

After being successively polished with 1.0, 0.3 and 0.05 μ m alumina powder, Glassy carbon electrodes (GCE) were ultrasonicated in deionized water and the absolute ethanol for 10 min several times. 4 mg of catalyst and 20 μ L of 5 wt. % Nafion solution were dispersed in 1 mL of a solution of deionized water and ethanol (1:1 in volume ratio). After stirring by ultrasonication for 20 min, a drop (10 μ L) of the suspension was added on the surface of GCE and allowed to dry in air. All the electrochemical measurements for HER were performed with an electrochemical station (Gamry Reference 600 Instruments, USA) in a traditional three-electrode system, using a Pt foil as the counter electrode, the modified GCE as the working electrode, and a Ag/AgCl (saturated KCl) as the reference electrode. The electrolyte for the measurement is 40 mL of 0.5 M H₂SO₄ (aq) (pH = 0.16) prepared using 18 M Ω deionized water. Before the measurement, the electrolyte is purged with N₂ for half an hour and N₂ is maintained through the test. All potentials reported in this paper were converted from

vs. Ag/AgCl to vs. RHE by adding a value of 0.22 V. Linear sweep voltammetry (LSV) polarization curves were conducted from 0.1 V to -0.5 V vs. RHE with a scan rate of 10 mV s^{-1} . Electric impedance spectroscopy (EIS) measurements were carried out at -0.2 V vs. RHE from 10^5 to 10^{-1} Hz with an AC potential amplitude of 5 mV. For comparison, blank GCE, MoS_2/MnS composite and the MoS_2 sample obtained without template were also measured under the identical conditions.

3. RESULTS AND DISCUSSION

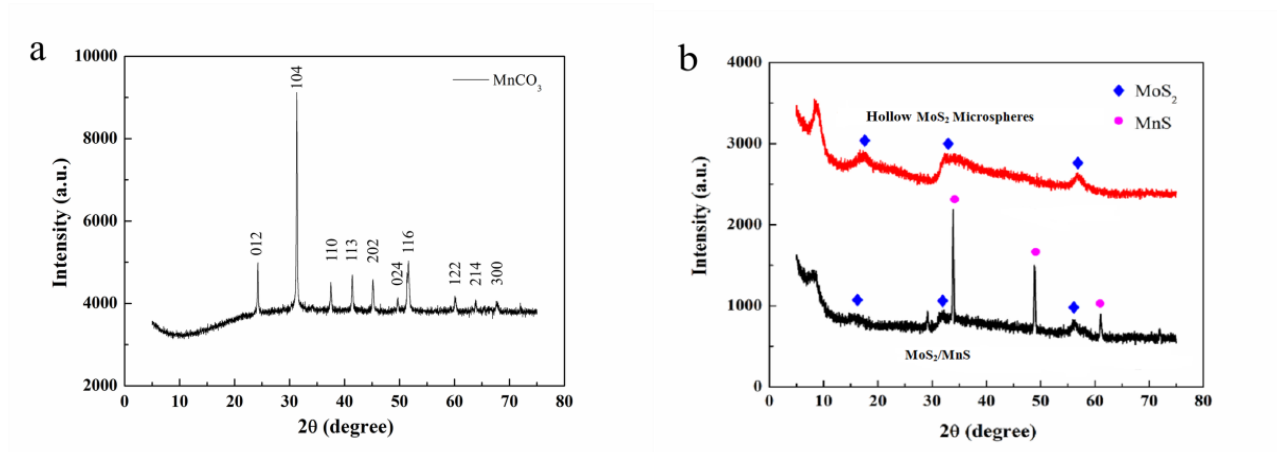
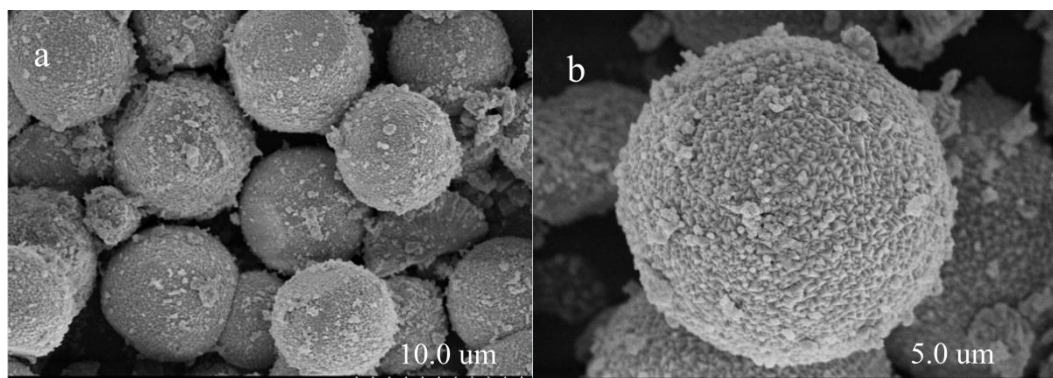


Figure 1. XRD patterns of the as-prepared MnCO_3 , MoS_2/MnS and hollow MoS_2 .

Fig. 1 shows the XRD patterns of the as-prepared MnCO_3 microspheres, MoS_2/MnS shell/core hybrid structures and MoS_2 microspheres. The peaks of MnCO_3 microspheres (Fig. 1a) are well assigned to pure phase of MnCO_3 (JCPDS Card 83-1763). After the process of hydrothermal, as shown in Fig. 1b, the peaks of MnS and MoS_2 begin to appear, indicating the transformation from MnCO_3 to MnS happens and MoS_2 is obtained through the hydrothermal reaction of $\text{Na}_2\text{MoO}_4 \cdot 2\text{H}_2\text{O}$ and L-cysteine. After the acid-treatment process, the peaks of MnS disappear and there only remains the peaks of MoS_2 , implying the removal of MnS during HCl treatment.



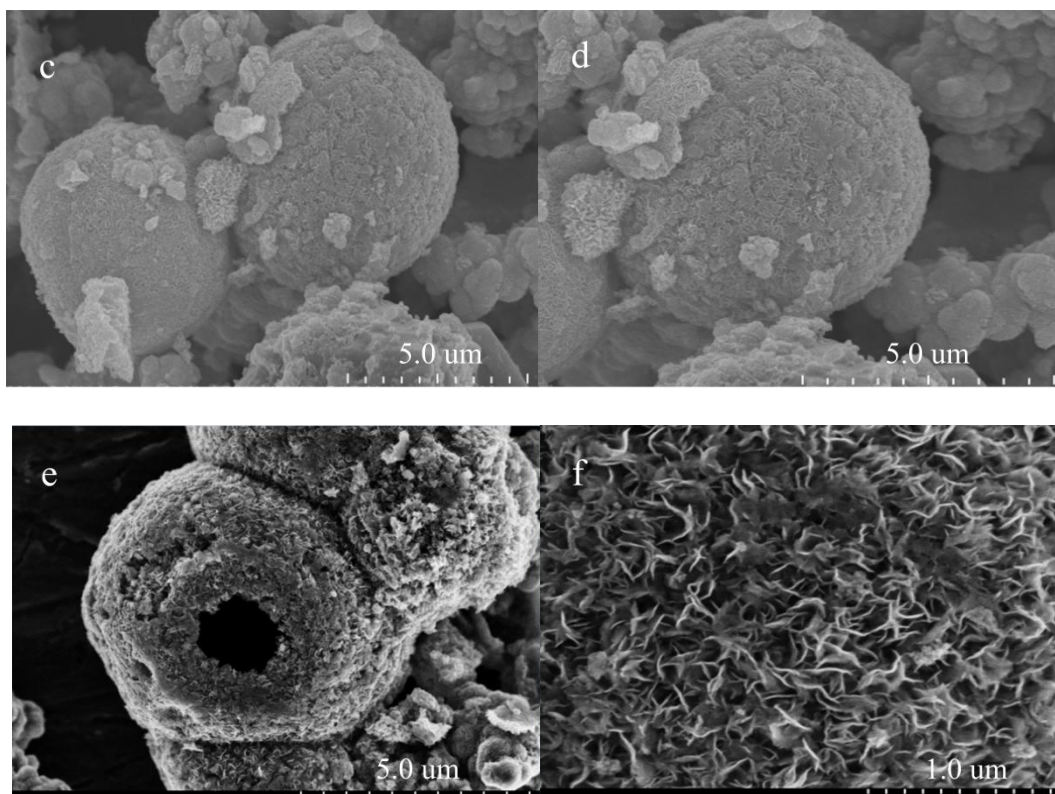
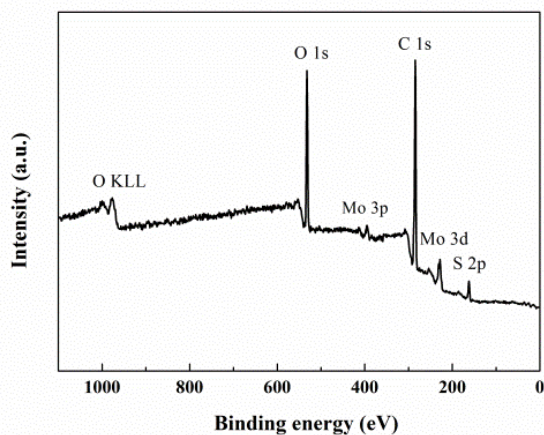


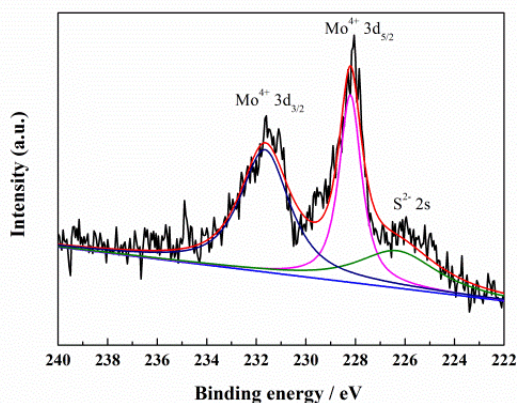
Figure 2. SEM images of the as-prepared MnCO_3 (a-b), MoS_2/MnS (c-d) and hollow MoS_2 (e-f).

Fig. 2a shows the SEM images of the as-prepared MnCO_3 , consisting of uniform microspheres, ranges from 9-11 μm , with an average size of 10 μm . An individual microsphere is exhibited in Fig. 2b. The detailed structure of MnCO_3 microspheres can be seen. On the surface of the MnCO_3 microsphere, a lot of triangular edges and corners are distributed, which are advantageous for the growth of MoS_2 . MoS_2 nanosheets are prepared by the hydrothermal reaction of $\text{Na}_2\text{MoO}_4 \cdot 2\text{H}_2\text{O}$ and L-cysteine, which acts as the reducing agent and the sulfur source. The multiple functional groups ($-\text{NH}_2$, $-\text{COO}-$ and $-\text{SH}$) of L-cysteine are helpful for the growth of MoS_2 nanosheets on the surface of MnCO_3 microspheres. As shown in Fig. 2c-d, after the hydrothermal process, MoS_2 nanosheets begin to appear and wrap around the MnCO_3 microspheres. The diameter of the MoS_2/MnS is nearly the same with the above MnCO_3 , indicating the obtained MoS_2 is thin. After the acid treatment, the core MnS was removed, as is shown in Fig. 2e-f. The hollow nature of MoS_2 can be clearly seen and the surface of MoS_2 is composed of many thin nanosheets, which mean the more edges and rims of the hollow MoS_2 microspheres.

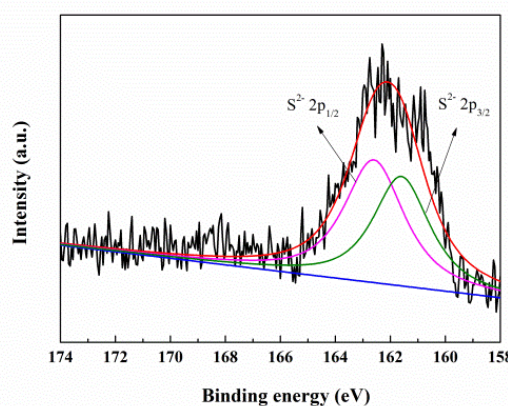
X-ray photoelectron spectroscopy (XPS) was measured to get the chemical state of hollow hierarchical MoS_2 . Fig. 3a shows the XPS survey spectrum of the hierarchical MoS_2 , confirming the existence of Mo, S. The high-resolution XPS spectra in Mo 3d and S 2p regions are shown in Fig. 3b and Fig. 3c. The peaks at 228.6 eV and 231.8 eV are consistency with the Mo (IV) $3d_{5/2}$ and Mo (IV) $3d_{3/2}$ [23-25] (Fig. 3b), the corresponding peaks for S^{2-} $2p_{3/2}$ and S^{2-} $2p_{1/2}$ are observed at 161.6 eV and 162.6 eV [26] (Fig. 3c). The peak at 226.3 eV next to Mo 3d region is the S 2s region [27]. The S: Mo stoichiometric ratio is 2.0, suggesting the chemical state of the surface is MoS_2 .



A



B



C

Figure 3. XPS (a) survey; (b) Mn 2p; (c) O 1s of hollow MoS₂.

In addition, the surface areas of the conventional MoS₂ and hollow MoS₂ microspheres are compared through the BET measurement as is shown in Table 1.

Table 1. BET surface area of different MoS₂ samples.

Samples	BET surface area (m ² g ⁻¹)
conventional MoS ₂	6.86
□ hollow MoS ₂ microspheres	9.50

The hollow MoS₂ microspheres exhibit the higher BET surface area of 9.50 m² g⁻¹, which is larger than that of the conventional MoS₂ (6.86 m² g⁻¹).

The electrochemical measurements for HER are conducted. LSV of MoS₂, MoS₂/MnS and hollow MoS₂ microspheres are compared in Fig. 4a. From the polarization curves, we can see that the hollow MoS₂ microspheres have a lowest overpotential with a value of -170 mV, which is much lower than the pure MoS₂ (-270 mV) and the MoS₂/MnS composite (-210 mV). The enhanced activity of hollow MoS₂ microspheres may be due to the increased edge sites through the dissolving process. As

is shown in Fig. 4b, the corresponding Tafel slopes of pure MoS₂, MoS₂/MnS and hollow MoS₂ microspheres are 182.3 mV dec⁻¹, 146.3 mV dec⁻¹ and 125.2 mV dec⁻¹, respectively.

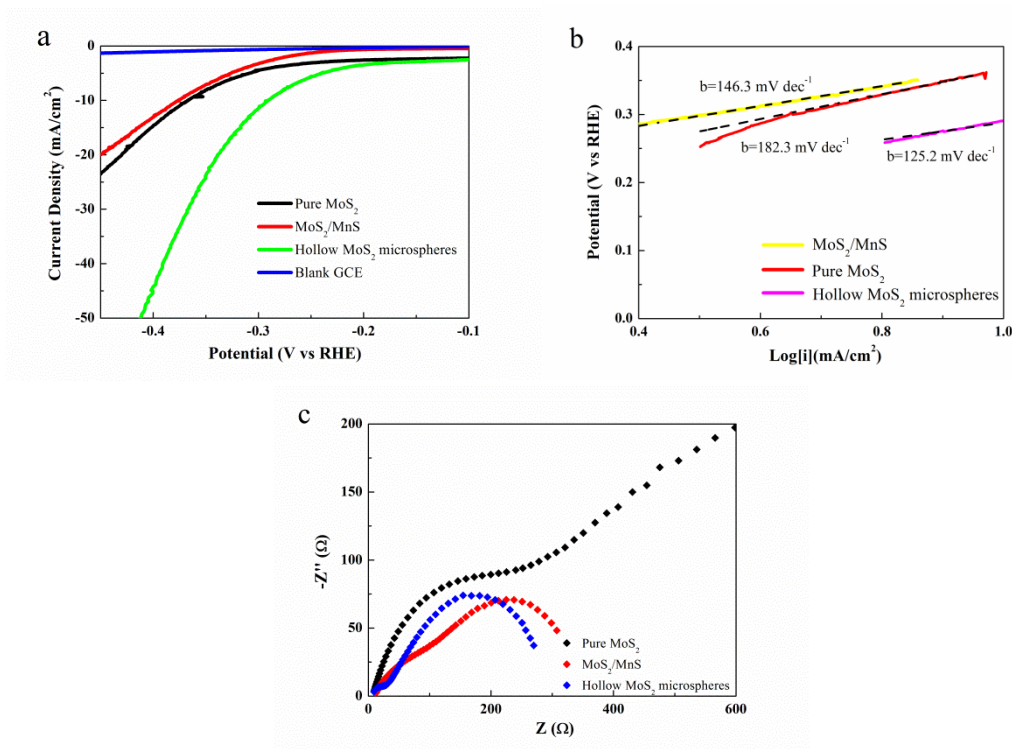


Figure 4. Electrocatalytic properties for HER of pure MoS₂, MoS₂/MnS and hollow MoS₂, (a) LSV (b) Tafel (c) EIS

Thus, the hollow MoS₂ microspheres have the lowest Tafel slope, leading to an advantage activity towards HER. Conductivity is another important issue to evaluate HER activity. EIS of the above three samples are compared in Fig. 4c. The hollow MoS₂ microspheres show a much smaller diameter of the semicircle than the pure MoS₂, indicating the enhanced conductivity of the MoS₂ obtained from the self-sacrificial template process.

4. CONCLUSIONS

A facile self-sacrificial template synthesis using MnCO₃ spheres as precursor has been used to prepare hollow MoS₂ microspheres. XRD show that pure MoS₂ has been obtained. SEM images show that hollow MoS₂ microspheres were consisted of many MoS₂ nanosheets, which can provide more exposed edges and rims. MnCO₃ as template is responsible for the synthesis of hollow MoS₂ microspheres. It is also confirmed that the electrocatalytic activity of hollow MoS₂ microspheres for HER has been enhanced compared to conventional MoS₂ nanoparticles. Therefore, template synthesis is advantageous choice for hollow MoS₂ microspheres with highly electrocatalytic activity.

ACKNOWLEDGEMENTS

This work is financially supported by the National Natural Science Foundation of China (U1162203 and 21106185) and the Fundamental Research Funds for the Central Universities (15CX05031A).

References

1. M. Gratzel, *Nature*, 414 (2001) 338
2. K.T. Lam, Y.J. Hsiao, L.W. Ji, T.H. Fang, W.S. Shih and J.N. Lin, *Int. J. Electrochem. Sci.*, 10 (2015) 3914
3. N.S. Lewis, *Science*, 315 (2007) 798
4. H. K. Abdel-Aa, *Int. J. Hydrogen Energy*, 40 (2015) 7568
5. L. Zhang, H.B. Wu, Y. Yan, X. Wang and X.W. Lou, *Energy Environ Sci.*, 7 (2014) 3302
6. C.Y. Tang, D.Z. Wang, Z.Z. Wu and B.H. Duan, *Int. J. Hydrogen Energy*, 40 (2015) 3229
7. Z.P. Yan, H.T. Wu, A.L. Han, X.S. Yu and P.W. Du, *Int. J. Hydrogen Energy*, 39 (2014) 13353
8. C.G. Morales-Guio, L.A. Stern and X.L. Hu, *Chem. Soc. Rev.*, 43 (2014) 6555
9. W.F. Chen, J.T. Muckerman and E. Fujita, *Chem. Commun.*, 49 (2013) 8896
10. M.A. Lukowski, A.S. Daniel, F. Meng, A. Forticaux, L.S. Li and S. Jin, *J. Am. Chem. Soc.*, 135 (2013) 10274
11. Z.Y. Yin, B. Chen, M. Bosman, X.H. Cao, J.Z. Chen, B. Zheng and H. Zhang, *Small*, 10 (2014) 3537
12. Y. Jiao, Y. Zheng, M. Jaroniec and S.Z. Qiao, *Chem. Soc. Rev.*, 44 (2015) 2060
13. X.P. Dai, K.L. Du, Z.Z. Li, H. Sun, Y. Yang, W. Zhang and X. Zhang, *Int. J. Hydrogen Energy*, 40 (2015) 8877
14. W. H. Hu, G.Q. Han, Y.R. Liu, B. Dong, Y.M. Chai, Y.Q. Liu and C.G. Liu, *Int. J. Hydrogen Energy*, 40 (2015) 6552
15. L. Cao, R. Wang, D. Wang, X. Li and H. Jia, *Mater. Lett.*, 160 (2015) 286
16. W. H. Hu, R. Yu, G.Q. Han, Y.R. Liu, B. Dong, Y.M. Chai, Y.Q. Liu and C.G. Liu, *Mater. Lett.*, 161 (2015) 120
17. S. Xu, Z. Lei and P. Wu, *J. Mater. Chem. A*, 3 (2015) 16337
18. L. Zhang, H.B. Wu, Y. Yan, X. Wang and X.W. Lou, *Energy Environ. Sci.*, 7 (2014) 3302
19. P. Wang, H. Sun, Y. Ji, W. Li and X. Wang, *Adv. Mater.*, 26 (2014) 964
20. N. Li, Y. Chai, Y. Li, Z. Tang, B. Dong, Y. Liu and C. Liu, *Mater. Lett.*, 66 (2012) 236
21. J. Li, D. Wang, H. Ma, Z. Pan, Y. Jiang, M. Li and Z. Tian, *Mater. Lett.*, 160 (2015) 550
22. J. Fei, Y. Cui, X. Yan, W. Qi, Y. Yang, K. Wang, Q. He and J. Li, *Adv. Mater.*, 20 (2008) 452
23. T. Weber, J.C. Muijsers and J.W. Niemantsverdriet, *J. Phys. Chem.*, 99 (1995) 9194
24. J.C. Muijsers, T. Weber, R.M. vanHardeveld, H.W. Zandbergen and J.W. Niemantsverdriet, *J. Catal.*, 157 (1995) 698
25. D. Merki, S. Fierro, H. Vrubel and X.L. Hu, *Chem. Sci.*, 2 (2011) 1262
26. T. Weber, J.C. Muijsers, J.H.M.C. vanWolput, C.P.J. Verhagen and J.W. Niemantsverdriet, *J. Phys. Chem.*, 100 (1996) 14144
27. H. Vrubel, X.L. Hu, *ACS Catalysis*, 3 (2013) 2002